

$B^{0(\pm)}$ decays into two vector mesons

Physical motivations and a general method for simulations

Z.J.Ajaltouni^{1*}, O.Leitner^{1,2†}, C.Rimbault^{1‡}

¹ *Laboratoire de Physique Corpusculaire de Clermont-Ferrand
IN2P3/CNRS Université Blaise Pascal
F-63177 Aubière Cedex France*

² *Department of Physics and Mathematical Physics and Special Research Centre for the
Subatomic Structure of Matter
Adelaide University
Adelaide 5005, Australia*

Abstract

In this paper, a complete description of the channels $B \rightarrow V_1 V_2$ is given. Emphasis is put on the determination of the dynamical density matrix which elements are computed according to the Wilson operator product expansions entering into the formulation of the weak effective hamiltonian.

Kinematical consequences related to the particular channel $B \rightarrow K^* \rho^0(\omega)$ are described in details.

*ajaltouni@in2p3.fr

†oleitner@physics.adelaide.edu.au

‡rimbault@clermont.in2p3.fr

1 Introduction

In a previous note [1], an exhaustive study of the channel simulations:

$$B \rightarrow V_1 V_2, \quad \gamma V, \quad PV, \quad PP,$$

($V = 1^-, P = 0^-$) has been performed by stressing the helicity formalism and its consequences. General formulas have been established, notably those giving the final angular distributions in the case of the production of two vector mesons decaying into pseudoscalar mesons.

The squared modulus of the decay amplitude has the following form:

$$|A|^2 \propto h_{\lambda, \lambda'} F_{\lambda, \lambda'}(\theta_1) G_{\lambda, \lambda'}(\theta_2, \phi), \quad (1)$$

where (summation over $\lambda(\lambda')$ is omitted):

- $h_{\lambda, \lambda'}$ is the matrix density element constructed from the weak effective hamiltonian H_w^{eff} taken between the initial state (B_0) and the final state f .
- $F_{\lambda, \lambda'}(\theta_1)$ and $G_{\lambda, \lambda'}(\theta_2, \phi)$ are the matrix elements related to the decays $V_1 \rightarrow a_1 + b_1$ and $V_2 \rightarrow a_2 + b_2$ respectively.
- θ_j is the polar angle of particle a_j in the rest frame of the resonance V_j while ϕ is the angular difference $\phi_2 - \phi_1$, where ϕ_j is the polar angle of a_j in V_j rest frame.

$\lambda(\lambda')$ being the helicity state of the vector mesons; $\lambda = -1, 0, +1$.

As it can be noticed, the essential parameters for the determination of the decay dynamics are the *unknown matrix elements* $h_{\lambda, \lambda'}$; while the two other ones, $F_{\lambda, \lambda'}(\theta_1)$ and $G_{\lambda, \lambda'}(\theta_2, \phi)$, are kinematic (or geometric) parameters because they are completely determined from the Wigner rotation matrices. The reader is referred to the note 99–051 for a full kinematic description of the B^0 decay and the physical significance of the angles $\theta_{1,2}$ and ϕ .

Before dealing with the mathematical determinations of the $h_{\lambda, \lambda'}$ elements, a simple justification of the two vector meson channel is given below.

2 Quantum numbers of the $V_1^0 V_2^0$ system

In the case of two vector meson B^0 decay, the most interesting case is the one related to neutral mesons supplemented by the condition $C|V_i^0\rangle = -|V_i^0\rangle$, where C is the charge conjugation operator and V_i^0 is a neutral vector meson *eigenstate* of C . Some examples of these channels are:

$$\rho^0 \rho^0, \quad J/\Psi \rho^0, \quad J/\Psi \Phi, \quad \Phi \Phi \dots$$

These vector mesons have, in addition, the *parity* quantum number equal to -1 . Noticing that the total angular momentum of the $V_1^0 V_2^0$ system: $\vec{J} = \vec{\ell} + \vec{S} = \vec{s}_B$ is equal

to zero and because the total spin $\vec{S} = \vec{s}_1 + \vec{s}_2$, with $s_1 = s_2 = 1$, the orbital angular momentum can have three different values: $\ell = S = 0, 1, 2$.

Thus, parity, charge conjugation and CP quantum numbers of the $V_1^0 V_2^0$ system can be computed:

$$P(V_1^0 V_2^0) = (-1)^2 (-1)^\ell, \quad C(V_1^0 V_2^0) = (-1)^2,$$

↓

$$CP(V_1^0 V_2^0) = (-1)^\ell.$$

We are led to the important result that the CP value of $V_1^0 V_2^0$ is a **mixing** of two different eigenvalues +1 and -1 whatever the initial state (B^0 or \bar{B}^0) is. A direct consequence of this result is that *CP symmetry is not an exact one*.

The above relation does not hold for reactions involving a neutral K^* like:

$$B_d^0 \rightarrow K^{*0} \rho^0, \quad J/\Psi K^{*0} \dots$$

because K^{*0} and \bar{K}^{*0} are two *distinct particles*; $C|K^{*0}\rangle = |\bar{K}^{*0}\rangle \neq |K^{*0}\rangle$.

However, it is worth noticing two interesting features for channels with an intermediate resonance like $K^{*0}(\bar{K}^{*0})$:

$$K^{*0} \rightarrow K^+ \pi^-, \quad K^0 \pi^0,$$

$$\bar{K}^{*0} \rightarrow K^- \pi^+, \quad \bar{K}^0 \pi^0.$$

The decay channels are in the ratio 2/3 and 1/3 respectively. On one hand, the sign of the charged kaon shows clearly the nature of the neutral K^* from which it comes and consequently the *flavour* of the original $B^0(\bar{B}^0)$. So, a neutral K^* decay is a direct way for B^0 *flavour tagging*.

On the other hand, when a neutral $K^{*0}(\bar{K}^{*0})$ decays into $K^0(\bar{K}^0)\pi^0$, the neutral kaon $K^0(\bar{K}^0)$ is not the true physical particle, because approximately 50% of the $K^0(\bar{K}^0)$ go into K_S^0 and 50% into K_L^0 respectively and the true *detectable* particle is K_S^0 which goes to $\pi^+\pi^-$.

Thus, in the special channel:

$$\begin{aligned} B^0(\bar{B}^0) &\rightarrow K^{*0}(\bar{K}^{*0})\rho^0, \\ &\rightarrow K_S^0\pi^0, \end{aligned}$$

tagging the original B^0 is no longer possible but, the $K_S^0\pi^0$ being a *common final state* to both B^0 and \bar{B}^0 , the above relation $CP = (-1)^\ell$ is still available [2].

In the following, emphasis will be put on the channels $K^{*0(\pm)}\rho^0(\omega)$ and the physical importance of the $\rho^0(\omega)$ mixing for the determination of **CP** violation.

$$B_d^0 \longrightarrow K^{*0} \rho^0(\omega)$$

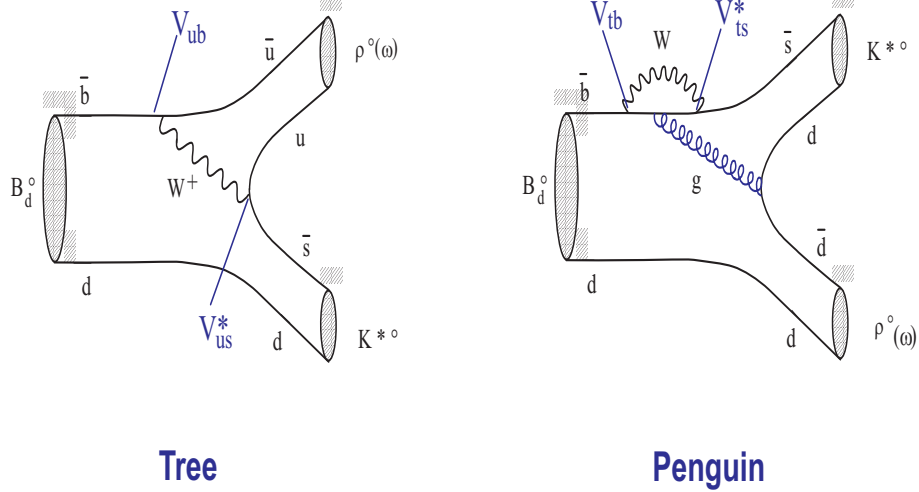


Figure 1: *Tree and Penguin diagrams for the decay $B^0 \rightarrow K^{*0} \rho^0(\omega)$.*

3 $\rho^0(\omega)$ mixing and its consequence

It is well known from hadronic physics that the neutral isovector ρ_8 and the isosinglet ω_8 mix together, leading to the "true" physical resonances ρ^0 and ω . On the phenomenological level, this mixing is made possible because of the existence of a common final state to both ρ^0 and ω decays [5]:

$$\begin{aligned} \rho^0 &\rightarrow \pi^+ \pi^-, & (BR \approx 100\%), \\ \omega &\rightarrow \pi^+ \pi^-, & (BR \approx 2.2\%). \end{aligned}$$

In the same framework, it has been established that the $\pi\pi$ final state interaction provides a phase shift δ which reaches 90° when the $\pi\pi$ invariant mass is at the ω pole ($M_\omega = 782 \text{ MeV}$) [6].

This interesting physical property has important consequences in the case where a ρ^0 resonance is produced in some $B^{0\pm}$ decays like:

$$B^0 \rightarrow K^{*0} \rho^0, \quad (\text{Fig.1})$$

$$B^+ \rightarrow K^{*+} \rho^0, \quad B^- \rightarrow K^{*-} \rho^0, \quad (\text{Fig.2})$$

These decays require both tree (T) and penguin (P) diagrams. As it is emphasized in reference [7], the amplitude A and \bar{A} respectively for B^+ and B^- decays can be set in the

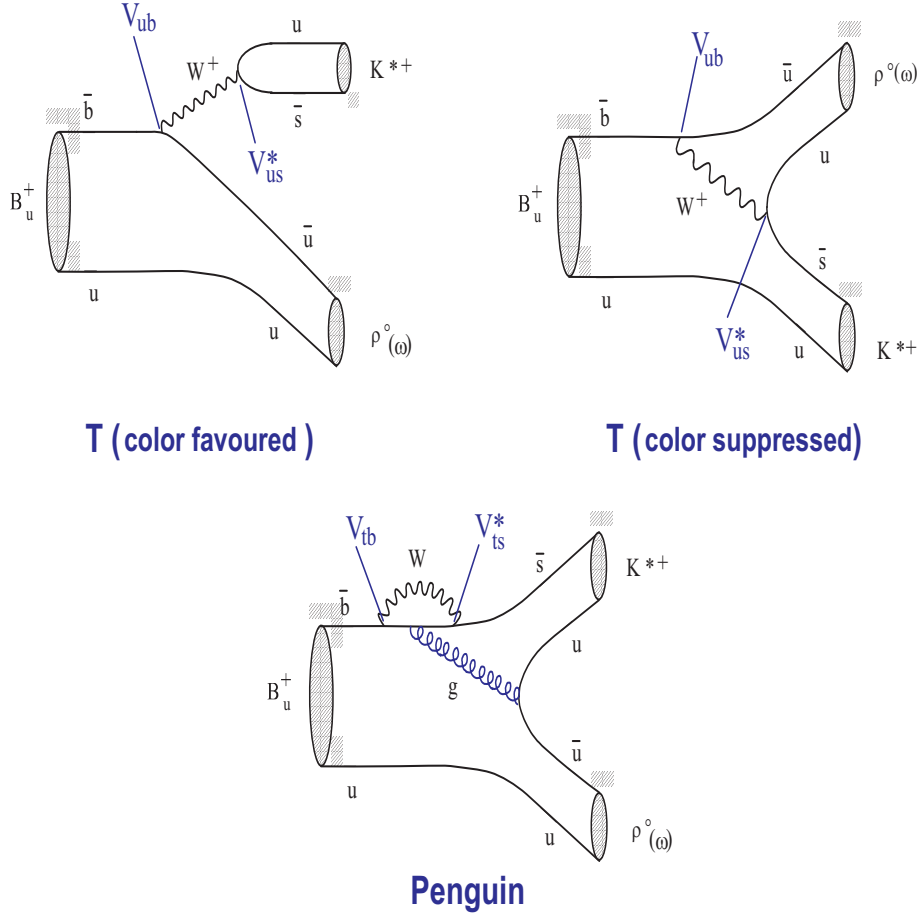


Figure 2: Tree and Penguin diagrams for the decay $B^+ \rightarrow K^{*+} \rho^0(\omega)$.

following form:

$$A = A^T + A^P = A^T(1 + r \exp(i\delta) \exp(i\phi)), \quad (2)$$

$$\bar{A} = \bar{A}^T + \bar{A}^P = A^T(1 + r \exp(i\delta) \exp(-i\phi)), \quad (3)$$

where:

$$r = \left| \frac{A^P}{A^T} \right|, \quad (4)$$

$$\bar{A}^T = A^T, \quad \bar{A}^P = |A^P| \exp(i\delta) \exp(-i\phi). \quad (5)$$

Expressions of A and \bar{A} displayed above suppose that final state interactions (FSI) arise essentially from the penguin diagrams; this hypothesis is supported by the fact that,

to order $G_F\alpha_s$ (G_F and α_s are respectively the Fermi constant and the QCD fine-structure constant), the *absorptive* part of the transition amplitude is obtained from the penguin diagrams [8].

In the special case of $\rho^0 - \omega$ mixing, another hypothesis is made using more intuitive arguments: the phase shift due to the mixing is included in the FSI and it is *predominating* at the ω pole, justifying the above expressions of A and \bar{A} that the phase shift δ is principally the one generated by the $\rho^0 - \omega$ mixing.

By CP transformation, the strong phase δ remains unchanged while the weak phase ϕ , which is related to the CKM matrix elements, changes sign. Thus, the asymmetry parameter a_{CP}^{dir} which can reveal *direct CP violation* can be deduced in the following way:

$$a_{CP}^{dir} = \frac{A^2 - \bar{A}^2}{A^2 + \bar{A}^2} = \frac{-2 \sin \delta \sin \phi}{1 + r^2 + 2r \cos \delta \cos \phi}. \quad (6)$$

It is straightforward to notice that the parameter a_{CP}^{dir} depends both on the strong phase *and* the weak phase and, consequently, the maximum value of a_{CP}^{dir} can be reached if $\sin \delta = 1$, which allows us to state that the strong final state interaction (FSI) among pions coming from the $\rho^0 - \omega$ decays *enhances* the direct CP violation in the vicinity of the resonance ω mass.

Simulation of the $\rho^0 - \omega$ mixing

A simple and phenomenological relation describing the amplitude of the $\rho^0 - \omega$ mixing is used for the Monte-carlo simulations [9]. In the ρ^0 Breit-Wigner, the (ρ^0) propagator is replaced by the following one:

$$\mathcal{A} = \frac{1}{s_\rho} + \frac{T_\omega}{T_\rho} \frac{\Pi_{\rho\omega}}{s_\rho s_\omega}, \quad (7)$$

where

- $1/s_V = 1/(s - M_V^2 + i\Gamma_V M_V)$ is the V resonance propagator, M_V and Γ_V being respectively the mass and the width of the resonance V .
- T_ω and T_ρ are respectively the ω and ρ production amplitudes.
- $\Pi_{\rho\omega}$ is the mixing parameter for which recent values come from e^+e^- annihilations: $\Re(\Pi_{\rho\omega}) = -3500 \pm 300 \text{ MeV}^2$ and $\Im(\Pi_{\rho\omega}) = -300 \pm 300 \text{ MeV}^2$.

Due to the same physical processes which enter into the production of the ρ^0 and ω resonances (they are both made out from $u\bar{u}$ and $d\bar{d}$ quark pairs with the same weight 1/2), it seems natural to choose $T_\omega/T_\rho = 1$. So, the squared mass distribution of the $\pi\pi$ system becomes simplified and it is given by:

$$d\sigma/dm^2 \propto |\mathcal{A}(\rho^0(\omega))|^2, \quad (8)$$

where \mathcal{A} is the amplitude of the two Breit-Wigner given above and m is the $\pi\pi$ invariant mass.

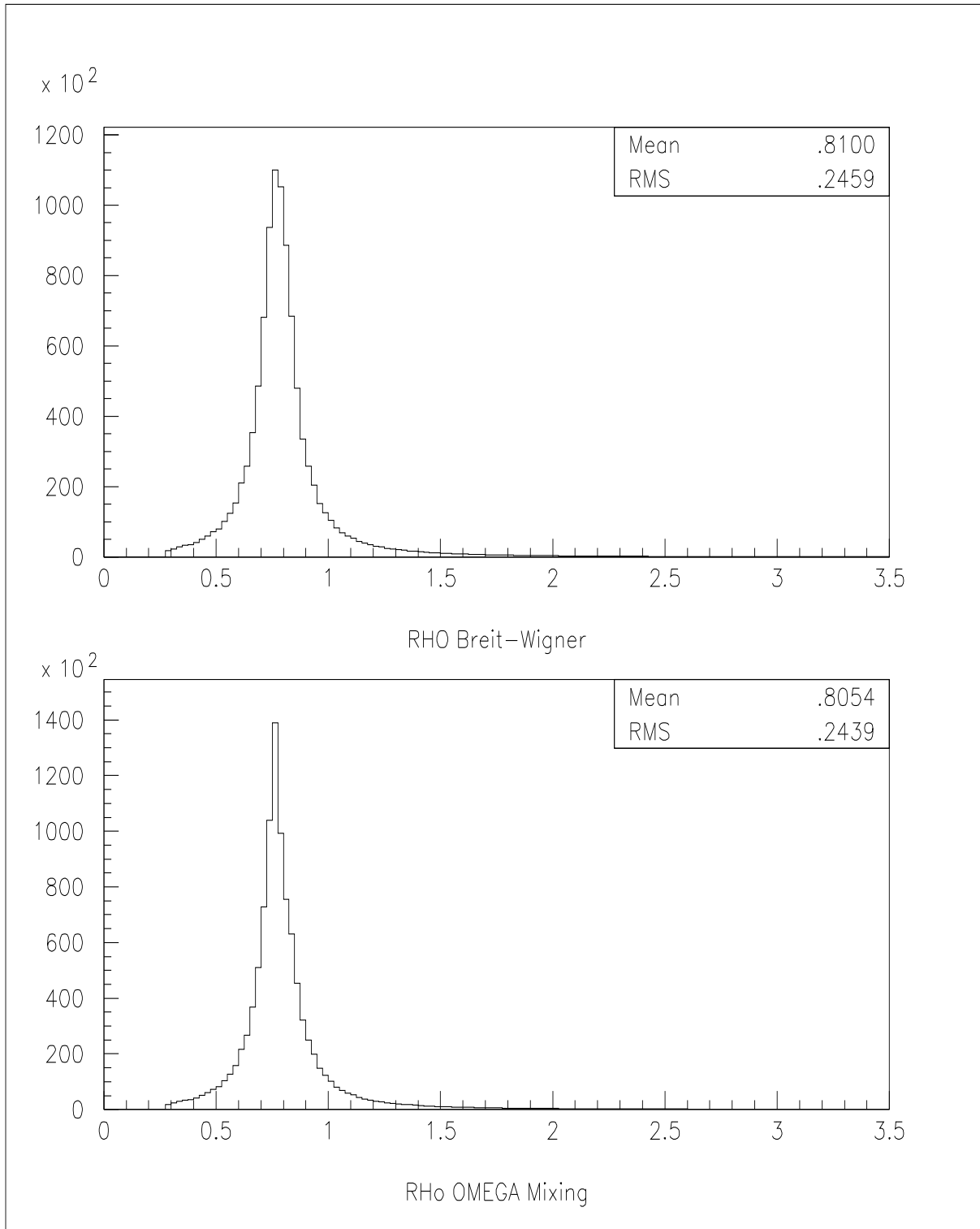


Figure 3: *Spectrum (in GeV/c^2) of ρ^0 Breit-Wigner (upper histogram) and $\rho^0 - \omega$ mixing (lower histogram).*

In Figure 3, are displayed the $\pi\pi$ invariant mass spectra for the ρ^0 Breit-Wigner and the $\rho^0 - \omega$ mixing respectively. Because of the very narrow ω width ($\Gamma_\omega = 8.44 \text{ MeV}$), we notice a high and narrow peak at the ω pole ($\approx 782 \text{ MeV}$).

4 Dynamics of the $B \rightarrow V_1 V_2$ decay

The formalism describing the $B^{0(\pm)}$ decay into two vector mesons is derived from the general formalism related to the hadronic weak decay of a heavy meson (or heavy quark). It is based on the new concepts introduced by the Heavy Quark Effective Theory (**HQET**) which involves additional symmetry due to the high mass of the heavy quark (b or c quark) [10]. Technical calculations require a weak effective hamiltonian, H_w^{eff} , by using the "Operator Product Expansions" (**OPE**) pioneered by Wilson and which involve field operators describing both *tree* and *penguin* diagrams, the last ones include both QCD and electroweak penguins (Figures 1 and 2).

The general form of H_w^{eff} is given by:

$$H_w^{eff} = \frac{G_F}{\sqrt{2}} \sum_{q=d,s} \left(V_{ub} V_{uq}^* (c_1 O_1 + c_2 O_2) - V_{tb} V_{tq}^* \sum_{i=3}^{10} c_i O_i \right), \quad (9)$$

where c_i are the Wilson coefficients and O_i are field operators with dimension $d \geq 4$; they are computed at an energy scale μ which is identified, here, with the b quark mass m_b .

In the case of charmless B decays, Wilson coefficients have been calculated by Buchalla et al [11]. These coefficients represent the *perturbative part* of the weak hamiltonian, they are estimated by the Renormalization Group techniques and their values depend on the renormalization scheme which is used. Their physical significance is the *weight* of each field operator $O_i(\mu)$ entering in the weak hamiltonian H_w^{eff} . From reference [12], the values of c_i which have been computed at the energy scale $\mu = m_b$ are:

$$\begin{aligned} c_1 &= -0.3125, & c_2 &= 1.1502, \\ c_3 &= 0.0174, & c_4 &= -0.0373, \\ c_5 &= 0.0104, & c_6 &= -0.0459, \\ c_7 &= -1.050 \times 10^{-5}, & c_8 &= 3.839 \times 10^{-4}, \\ c_9 &= -0.0101, & c_{10} &= 1.959 \times 10^{-3}. \end{aligned} \quad (10)$$

The first two coefficients, c_1 and c_2 , are related to the *tree* diagrams and they show clearly their dominance with respect to the *penguin* ones. Coefficients $c_3 - c_6$ correspond to QCD penguin operators while $c_7 - c_{10}$ are related to the EW ones.

However, those values of c_i must be modified when renormalization of operator O_i at one-loop order is taken into account.

Detailed expressions of operators $O_i(\mu)$ and their physical interpretation are given in reference [13].

Thus, a general form for the weak decay amplitude into a final state f can be expressed like:

$$A(B^0 \rightarrow f) = \langle f | H_w^{eff} | B^0 \rangle = \frac{G_F}{\sqrt{2}} \sum_{i=1}^{10} \sum_{q=d,s} \lambda_q^i c_i(\mu) \langle f | O_i(\mu) | B^0 \rangle, \quad (11)$$

where λ_q^i is the product of two CKM matrix elements: $V_{ub}V_{uq}^*$ (for $i = 1, 2$) or $(V_{tb}V_{tq}^*)$ (for $i = 3, \dots, 10$).

The hadronic matrix elements $\langle f | O_i(\mu) | B^0 \rangle$ represent the *non-perturbative contribution* to the amplitude $A(B^0 \rightarrow f)$. Usually, they are estimated according to some specific models: Non Relativistic Quark Model (NRQM), Form Factor models (BSW) and especially the Lattice QCD calculations.

In the following, calculation of the hadronic matrix elements is performed in the framework of the BSW model [14] from which form factors are derived by the knowledge of the hadronic wave functions for both initial and final states.

5 Determination of the density-matrix elements

The B^0 decay into two vector mesons requires the helicity formalism which has been intensively used in the previous paper [1]. To each vector meson (spin 1) is assigned a set of three polarization 4-vectors defined in this way:

$$\epsilon_1 = (0, \vec{\epsilon}_1), \quad \epsilon_2 = (0, \vec{\epsilon}_2), \quad \epsilon_3 = \left(|\vec{k}|/m, E\hat{k}/m \right), \quad (12)$$

and verifying the following relations:

$$\epsilon_i^2 = -1, \quad \epsilon_i \cdot \epsilon_j = 0, \quad \text{with } i \neq j, \quad (13)$$

where m, E, \vec{k} are respectively the mass, the energy and the momentum of the vector meson; \hat{k} is defined as the unit vector along the vector momentum, $\hat{k} = \vec{k}/|\vec{k}|$.

The three vectors $\vec{\epsilon}_1, \vec{\epsilon}_2$ and $\vec{\epsilon}_3 = E\hat{k}/m$ form an orthogonal basis; ϵ_1 and ϵ_2 are called the *transverse polarization* vectors while $\vec{\epsilon}_3$ is the *longitudinal polarization* one.

From that basis, an *helicity basis* is defined according to:

$$\epsilon(+)=\frac{(\epsilon_1+i\epsilon_2)}{\sqrt{2}}, \quad \epsilon(-)=\frac{(\epsilon_1-i\epsilon_2)}{\sqrt{2}}, \quad \epsilon(0)=\epsilon_3. \quad (14)$$

These 4-vectors are *eigenvectors* of the helicity operator \mathcal{H} with the eigenvalues $\lambda = +1, -1$ and 0 respectively. For a clear account of the helicity basis for a spin 1 particle, the reader can consult the book of Dewitt-Smith [15].

In the case of two vector mesons coming from the B decay, their 4-momenta are defined in the B rest frame and their corresponding polarization vectors are *correlated* because $\hat{k}_1 = -\hat{k}_2$. For an explicit calculation of their spatial components, see the appendix A.

The weak hadronic amplitude is then decomposed on the helicity basis according to the general formalism developed by the authors BSW [14]. This method allows one to obtain two interesting results:

- the contribution of the *tree* and *penguin* operators to the global amplitude via the helicity states.
- the total contribution of each helicity state.

A way of illustrating this method is to study the channel: $B^0(\bar{B}^0) \rightarrow K^{*0}(\bar{K}^{*0})\rho^0$.

(i) First of all, the mass of each resonance (K^{*0} and ρ^0) is generated according to a relativistic Breit-Wigner:

$$\frac{d\sigma}{dM^2} = C \frac{\Gamma_R M_R}{(M^2 - M_R^2)^2 + (\Gamma_R M_R)^2}, \quad (15)$$

C being a normalization constant.

(ii) The weak hadronic matrix element is expressed as the **sum** of three helicity matrix elements; each one of the form, $H_\lambda = \langle V_1 V_2 | H_w^{eff} | B \rangle$, is defined by gathering all the Wilson coefficients of both tree and penguin operators. Linear combinations of those coefficients arise like: c_{t1}^ρ , c_{p1}^ρ , and c_{p2}^ρ (see Appendix B) and the *helicity amplitude* H_λ gets the following expression:

$$\begin{aligned} H_\lambda = & \left(V_{ub} V_{us}^* c_{t1}^\rho - V_{tb} V_{ts}^* c_{p2}^\rho \right) \left\{ \beta_1 \varepsilon_{\alpha\beta\gamma\delta} \epsilon_K^{*\alpha}(\lambda) \epsilon_\rho^{*\beta}(\lambda) P_B^\gamma P_K^\delta \right. \\ & \left. + i \left(\beta_2 \epsilon_K^*(\lambda) \epsilon_\rho^*(\lambda) - \beta_3 (\epsilon_K^*(\lambda) \cdot P_B) (\epsilon_\rho^*(\lambda) \cdot P_B) \right) \right\} \\ & + \left(- V_{tb} V_{ts}^* c_{p1}^\rho \right) \left\{ \beta_4 \varepsilon_{\alpha\beta\gamma\delta} \epsilon_\rho^{*\alpha}(\lambda) \epsilon_K^{*\beta}(\lambda) P_B^\gamma P_\rho^\delta, \right. \\ & \left. + i \left(\beta_5 \epsilon_\rho^*(\lambda) \epsilon_K^*(\lambda) - \beta_6 (\epsilon_\rho^*(\lambda) \cdot P_B) (\epsilon_K^*(\lambda) \cdot P_B) \right) \right\} \end{aligned} \quad (16)$$

with:

- $\varepsilon_{\alpha\beta\gamma\delta}$: antisymmetric tensor in the Minkowski space.
- $\beta_{1,4} = \frac{G_F}{2} f_{\rho,K} m_{\rho,K^*} \frac{2}{m_B + m_{K^*,\rho}} V^{B \rightarrow K^*,\rho}(m_{\rho,K^*}^2)$.
- $\beta_{2,5} = \frac{G_F}{2} f_{\rho,K} m_{\rho,K^*} (m_B + m_{K^*,\rho}) A_1^{B \rightarrow K^*,\rho}(m_{\rho,K^*}^2)$.
- $\beta_{3,6} = \frac{G_F}{2} f_{\rho,K} m_{\rho,K^*} \frac{2}{m_B + m_{K^*,\rho}} A_2^{B \rightarrow K^*,\rho}(m_{\rho,K^*}^2)$.
- f_K, f_ρ : respectively K^{*0} and ρ^0 decay constants.
- $V^{B \rightarrow K^*,\rho}, A_i^{B \rightarrow K^*,\rho}$: respectively Vector and Axial form factors (see Appendix C).
- $\epsilon_{K,\rho}(\lambda)$: K^{*0}, ρ^0 polarization vectors expressed in the B rest frame.

It is worth noticing that the tensorial terms which enter H_λ become simplified in the B rest frame because the B 4-momentum is given by $P_B = (m_b, \vec{0})$. Then, using the orthogonality properties of $\epsilon_j(\lambda)$, the helicity amplitude H_λ acquires a much simpler expression than above:

$$H(\lambda) = iB(\lambda)(V_{ub}V_{us}^*c_{t_1}^\rho - V_{tb}V_{ts}^*c_{p_2}^\rho) + iC(\lambda)(-V_{tb}V_{ts}^*c_{p_1}^\rho), \quad (17)$$

with:

$$\begin{aligned} B(0) &= \beta_2 \frac{m_B^2 - (m_K^2 + m_\rho^2)}{2m_K m_\rho} - \beta_3 \frac{|\vec{p}|^2 m_B^2}{m_K m_\rho}, \\ C(0) &= \beta_5 \frac{m_B^2 - (m_K^2 + m_\rho^2)}{2m_K m_\rho} - \beta_6 \frac{|\vec{p}|^2 m_B^2}{m_K m_\rho}, \\ B(\pm 1) &= \mp \beta_1 m_B |\vec{p}| - \beta_2, \\ C(\pm 1) &= \mp \beta_4 m_B |\vec{p}| - \beta_5, \end{aligned} \quad (18)$$

$|\vec{p}|$ being the common momentum to V_1 and V_2 particles in the B rest frame.

(iii) Expressing the CKM matrix elements according to Wolfenstein parametrization [16]:

$$V_{CKM} = \begin{bmatrix} 1 - \frac{\lambda^2}{2} & \lambda & A\lambda^3(\rho - i\eta) \\ -\lambda & 1 - \frac{\lambda^2}{2} & A\lambda^2 \\ A\lambda^3(1 - \rho - i\eta) & -A\lambda^2 & 1 \end{bmatrix} + O(\lambda^4), \quad (19)$$

where we use[17]:

$$\begin{aligned} A &= 0.815, & \lambda &= 0.2205: \text{ well known} \\ 0.09 &< \rho < 0.254, & 0.323 &< \eta < 0.442. \end{aligned}$$

Taking into account the preceding relations, we arrive at the final form for the amplitudes H_λ :

$$\begin{aligned} H\left(\begin{smallmatrix} 0 \\ \pm 1 \end{smallmatrix}\right) &= A\lambda^2 \left\{ \left[\left(\eta\lambda^2 c_{t_1}^\rho - \Im m(c_{p_2}^\rho) \right) B\left(\begin{smallmatrix} 0 \\ \pm 1 \end{smallmatrix}\right) - \Im m(c_{p_1}^\rho) C\left(\begin{smallmatrix} 0 \\ \pm 1 \end{smallmatrix}\right) \right] \right. \\ &\quad \left. + i \left[\left(\rho\lambda^2 c_{t_1}^\rho + \Re e(c_{p_2}^\rho) \right) B\left(\begin{smallmatrix} 0 \\ \pm 1 \end{smallmatrix}\right) + \Re e(c_{p_1}^\rho) C\left(\begin{smallmatrix} 0 \\ \pm 1 \end{smallmatrix}\right) \right] \right\}, \end{aligned} \quad (20)$$

from which the density-matrix elements $h_{\lambda,\lambda'}$ can be derived automatically;
 $\Rightarrow h_{\lambda,\lambda'} = H_\lambda H_{\lambda'}^*$.

Due to the *hermiticity* of the matrix $(h_{\lambda,\lambda'})$, only six elements must be calculated and, furthermore, a normalization condition is applied:

$$N (h_{++} + h_{00} + h_{--}) = 1, \quad (21)$$

(N being the normalization constant) which makes easier the comparison of the modulus of the different matrix elements.

In the next histograms (Fig.4 - Fig.9) are displayed the spectra of $h_{\lambda,\lambda'}$ for different values of the Wolfenstein parameters ρ and η . In our study, these spectra are obtained for the four couples of values: (0.09, 0.323); (0.09, 0.442); (0.254, 0.323) and (0.254, 0.442). But, due to the fact that some density matrix elements do not vary too much with ρ and η , in most cases only the spectra corresponding to the first couple of values are shown. All the histograms correspond to a sample of 20000 generated events.

It is important to notice that large spectrum of values for $h_{\lambda,\lambda'}$ are obtained and *not single ones* because of the broad range of both the ρ^0 resonance mass and the common momentum $|\vec{p}|$ (see the analytical expressions of $B(\lambda)$ and $C(\lambda)$ given above).

- Whatever the values of ρ and η are, the dominant value of $h_{++} = |H_{+1}|^2$ is $\leq 10^{-2}$, numerical result which is proved too by complete analytical calculations. Thus the dominant polarization state is the **longitudinal** one because $h_{00} = |H_0|^2 \geq 60\%$, its mean value being around 85% (Fig.4).
- Due to the tiny value of $|H_{+1}|$, the modulus of the non-diagonal elements $h_{+-} = H_+H_-^*$ and $h_{+0} = H_+H_0^*$ are usually smaller than 0.2; while the modulus of $h_{-0} = H_-H_0^*$ can reach 0.5 (Fig.5).

Fig.6 and Fig.7 display the variations of the diagonal matrix elements h_{--} , h_{00} and h_{++} with respect to the four sets of ρ and η values: it can be seen that h_{++} has always a tiny value and h_{00} is always dominant. Other physical features appear: h_{00} is very *sensitive* to the parameter η ; its spectrum is rather wide for $\eta = 0.323$, while it is bounded between 0.8 and 1.0 for $\eta = 0.442$. For a fixed value of η , no noticeable variation with the parameter ρ is seen.

Fig.8 shows the real and imaginary parts of the non-diagonal elements h_{-0} , h_{+-} , h_{+0} respectively for $\rho = 0.09$ and $\eta = 0.323$. It is worth noticing that both real and imaginary parts of h_{+-} and h_{+0} are too small and close to zero.

Due to the importance of h_{+-} matrix element in the ϕ angle distribution (see Section 6), a full study of both real and imaginary parts of h_{+-} has been done. Fig.9 shows the corresponding spectra according to the values of ρ and η . It can be deduced that the real and imaginary parts have very similar distributions and both are dominated by small values (≤ 0.05).

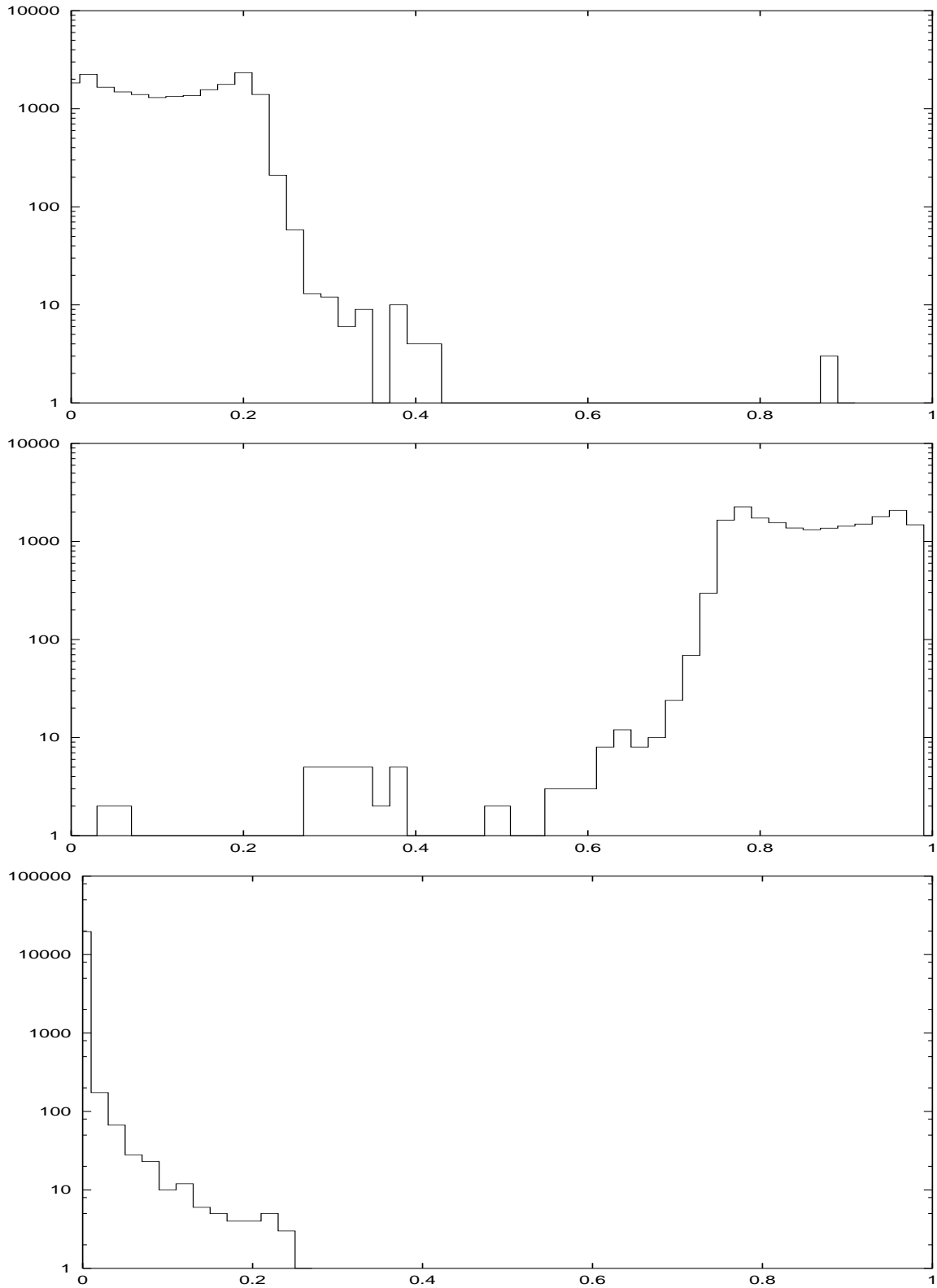


Figure 4: Diagonal matrix elements: h_{--}, h_{00}, h_{++} respectively for $\rho = 0.09, \eta = 0.323$.

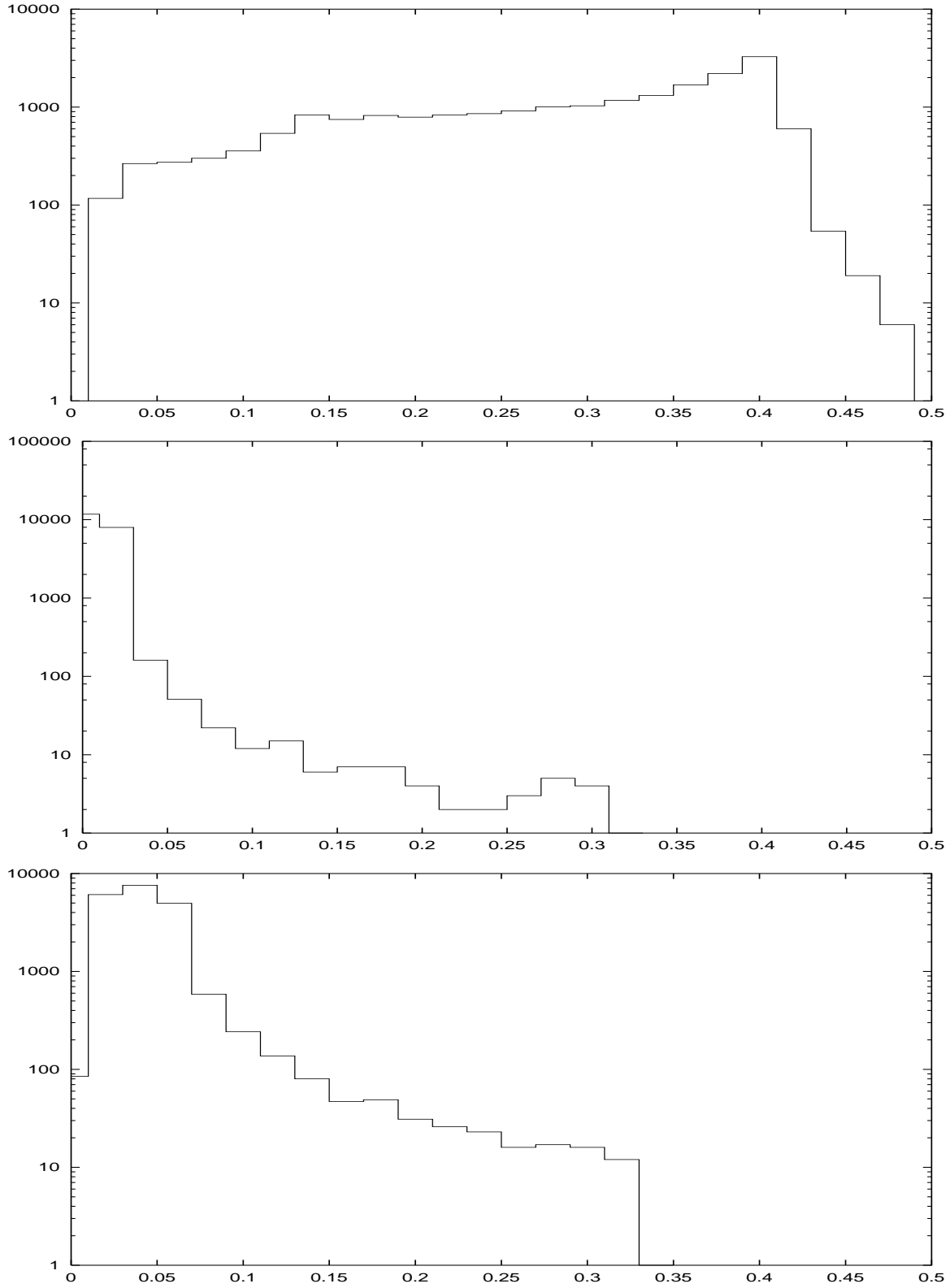


Figure 5: Modulus of non diagonal matrix elements: h_{0-}, h_{+-}, h_{+0} respectively for $\rho = 0.09, \eta = 0.323$.

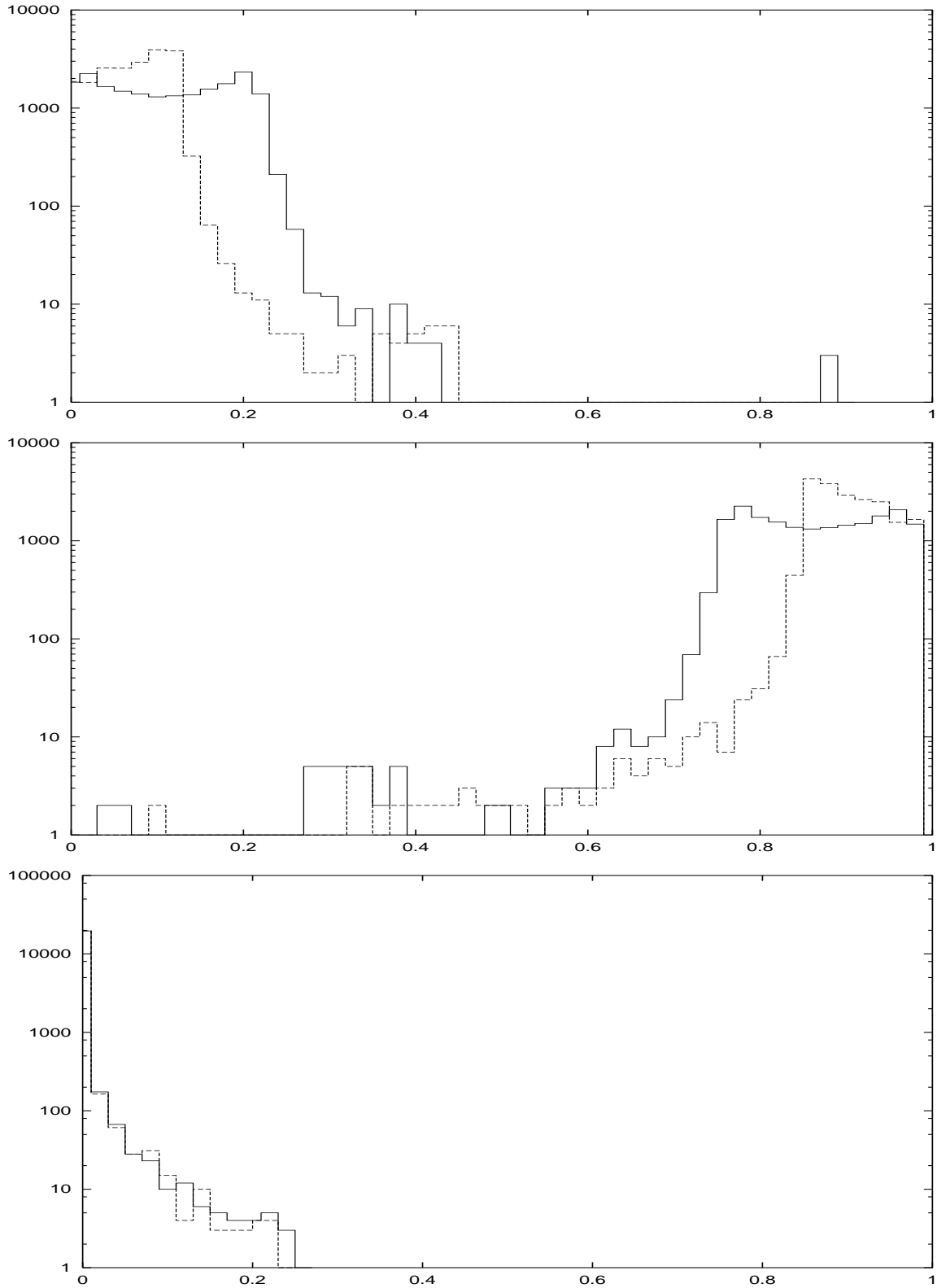


Figure 6: Variations of h_{--}, h_{00}, h_{++} according to Wolfenstein parameters: $\rho = 0.09, \eta = 0.323$ (full line) and $\eta = 0.442$ (dashed line).

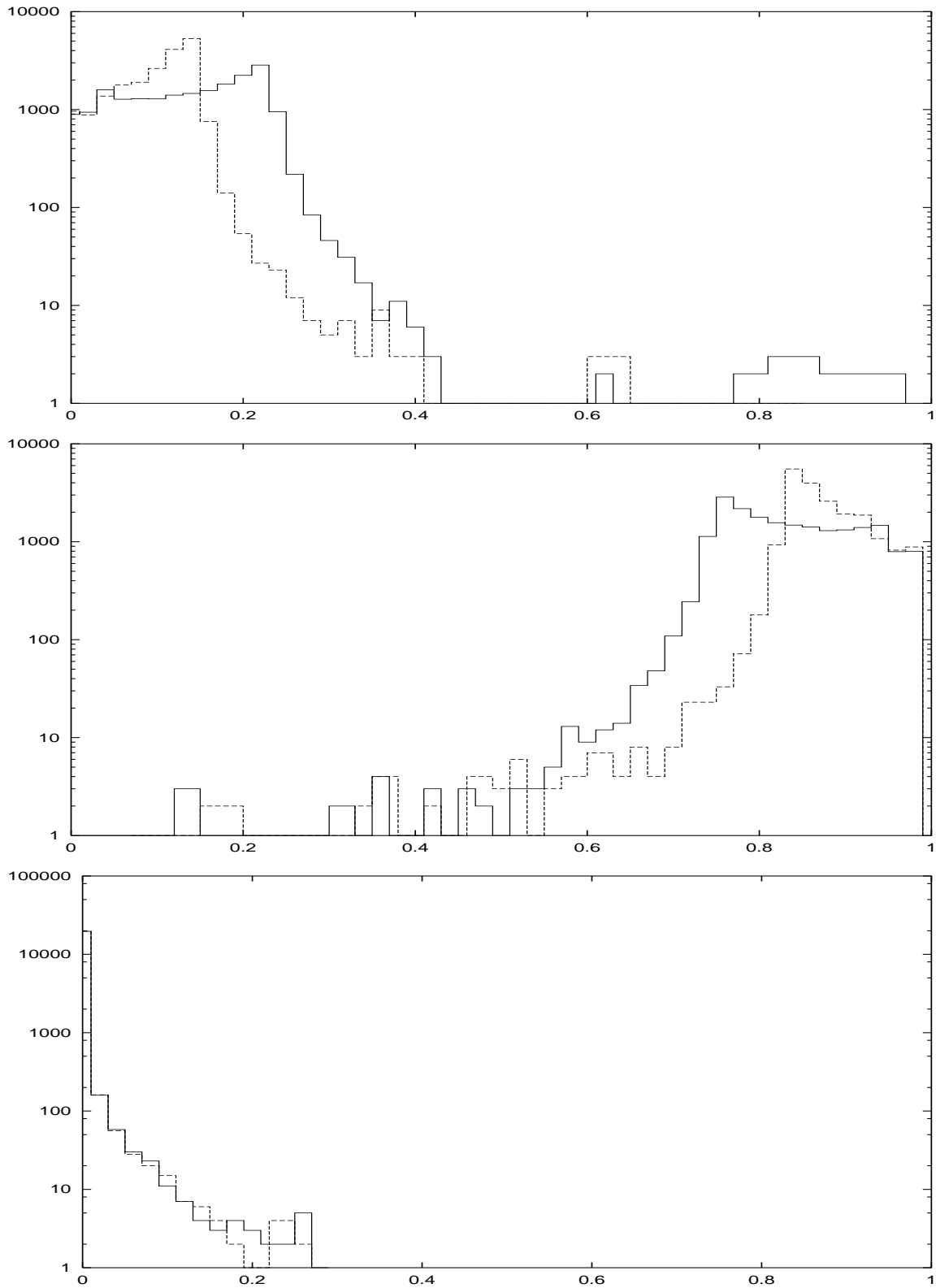


Figure 7: Variations of h_{--}, h_{00}, h_{++} according to Wolfenstein parameters: $\rho = 0.254, \eta = 0.323$ (full line) and $\eta = 0.442$ (dashed line).

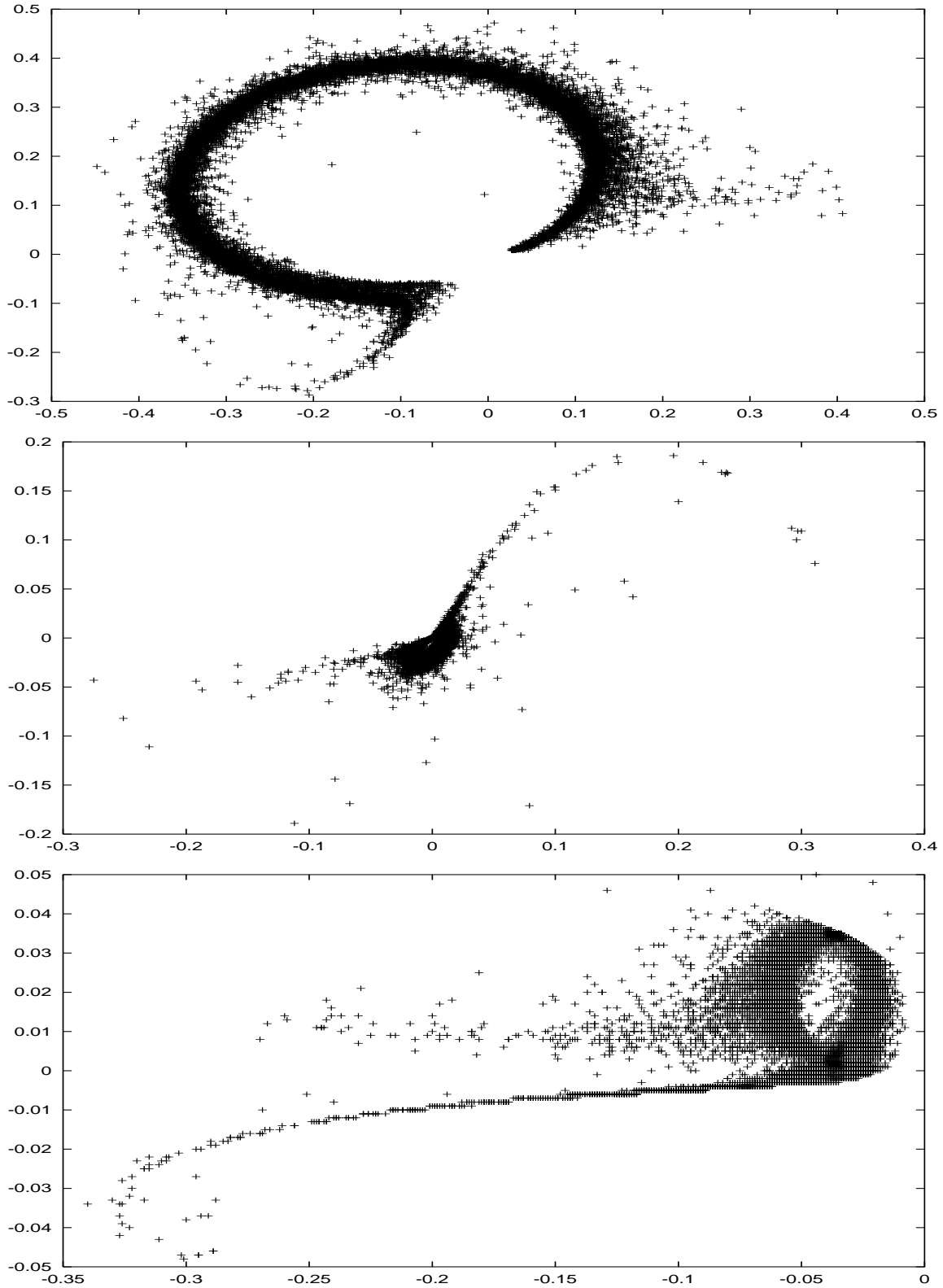


Figure 8: *Imaginary part vs Real part of matrix elements h_{0-}, h_{+-}, h_{+0} respectively for $\rho = 0.09, \eta = 0.323$.*

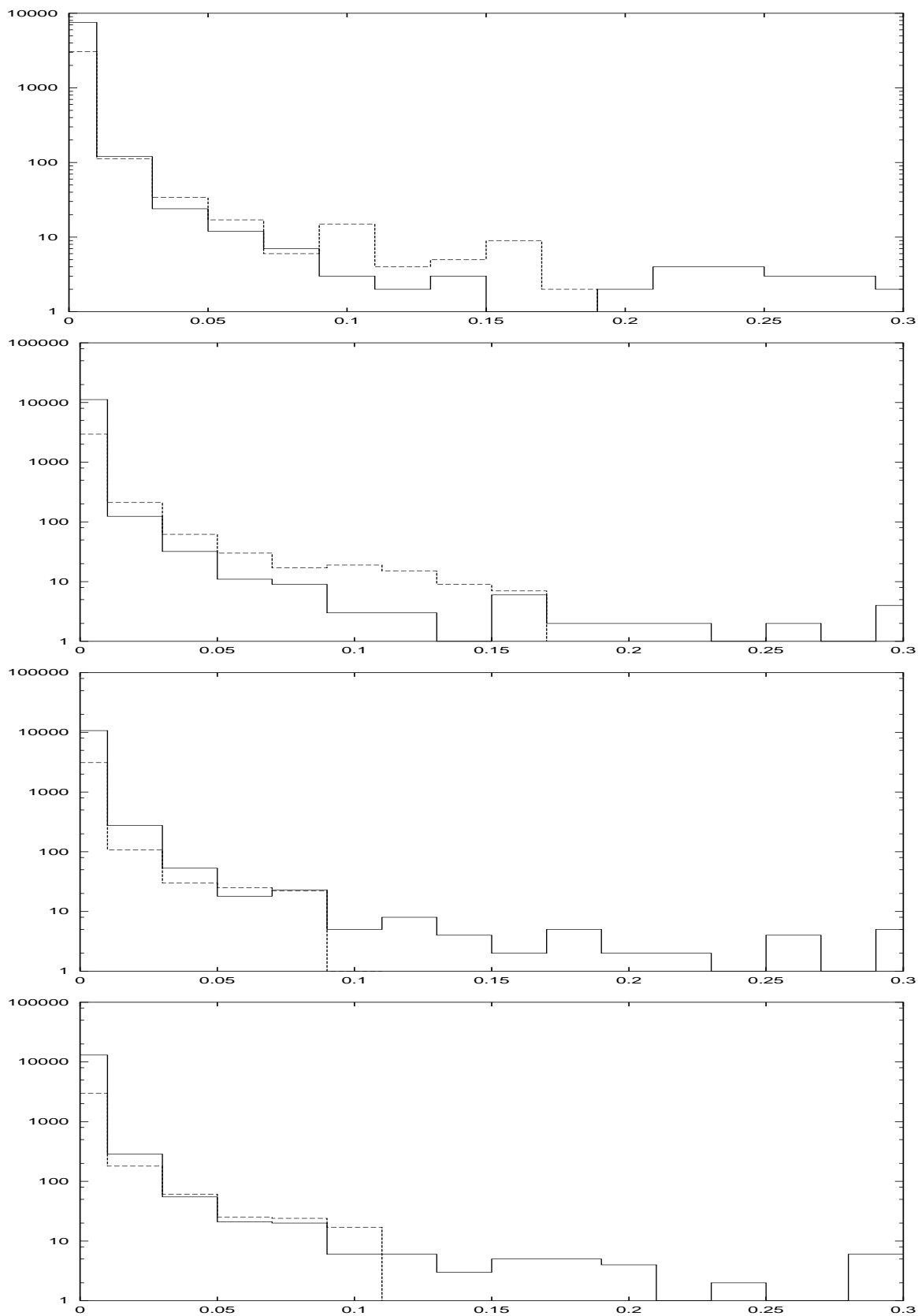


Figure 9: Real part (full line) and Imaginary part (dashed line) of h_{+-} matrix element for $(\rho, \eta) = (0.09, 0.323); (0.09, 0.442); (0.254, 0.323)$ and $(0.254, 0.442)$ respectively.

6 Decays of vector mesons $V_1 V_2$ into two pseudoscalar mesons

The matrix elements derived above allow us to compute the *degrees of polarization* of each resonance like K^* or ρ^0 . The angular distributions of the pseudoscalar mesons in each V_i rest frame depend on:

- (i) the spin 1 of the vector meson V_i .
- (ii) the weight of each helicity state.
- (iii) the correlations among the helicity states of the two vector mesons.

Complete analytical expression of the final angular distributions is the following one:

$$\begin{aligned} \frac{d^3\Gamma}{d\cos\theta_1 d\cos\theta_2 d\phi} &\propto (h_{++} + h_{--})\sin^2\theta_1\sin^2\theta_2/4 + h_{00}\cos^2\theta_1\cos^2\theta_2 \\ &+ (\Re(h_{+0})\cos\phi - \Im(h_{+0})\sin\phi + \Re(h_{0-})\cos\phi - \Im(h_{0-})\sin\phi) \sin 2\theta_1\sin 2\theta_2/4 \\ &+ (\Re(h_{+-})\cos 2\phi - \Im(h_{+-})\sin 2\phi) \sin^2\theta_1\sin^2\theta_2/2. \end{aligned} \quad (22)$$

Angles θ_1 , θ_2 and ϕ have been defined in Section 1.

Explicit angular distributions for polar and azimuthal angles can be derived from the relation above. It is interesting to notice that, due to the pseudoscalar nature of the final particles, angles θ_1 and θ_2 have the *same* distributions:

- $d\sigma/d\cos\theta_{1,2} \propto (3h_{00} - 1) \cos^2\theta_{1,2} + (1 - h_{00})$.
- $d\sigma/d\phi \propto (1 + 2(\Re(h_{+-}) \cos 2\phi - \Im(h_{+-}) \sin 2\phi))$.

In Fig.10 are displayed respectively the $\cos\theta$ distribution and the azimuthal angle ϕ one. Some comments on these curves are necessary:

- The $\cos\theta$ distribution is practically the same whatever the values of ρ and η are; no sensitivity to particular values of ρ and η is seen.
- As far as angle ϕ is concerned, its distribution depends on the matrix element h_{+-} . Despite the fact that $\Re(h_{+-})$ and $\Im(h_{+-})$ do not exhibit sensitive differences (see Fig.9), those parameters present some dependence upon ρ and η : full curve corresponds to $\rho = 0.09, \eta = 0.323$; while dashed one is related to $\rho = 0.254, \eta = 0.442$. A visible discrepancy among these two curves is seen.

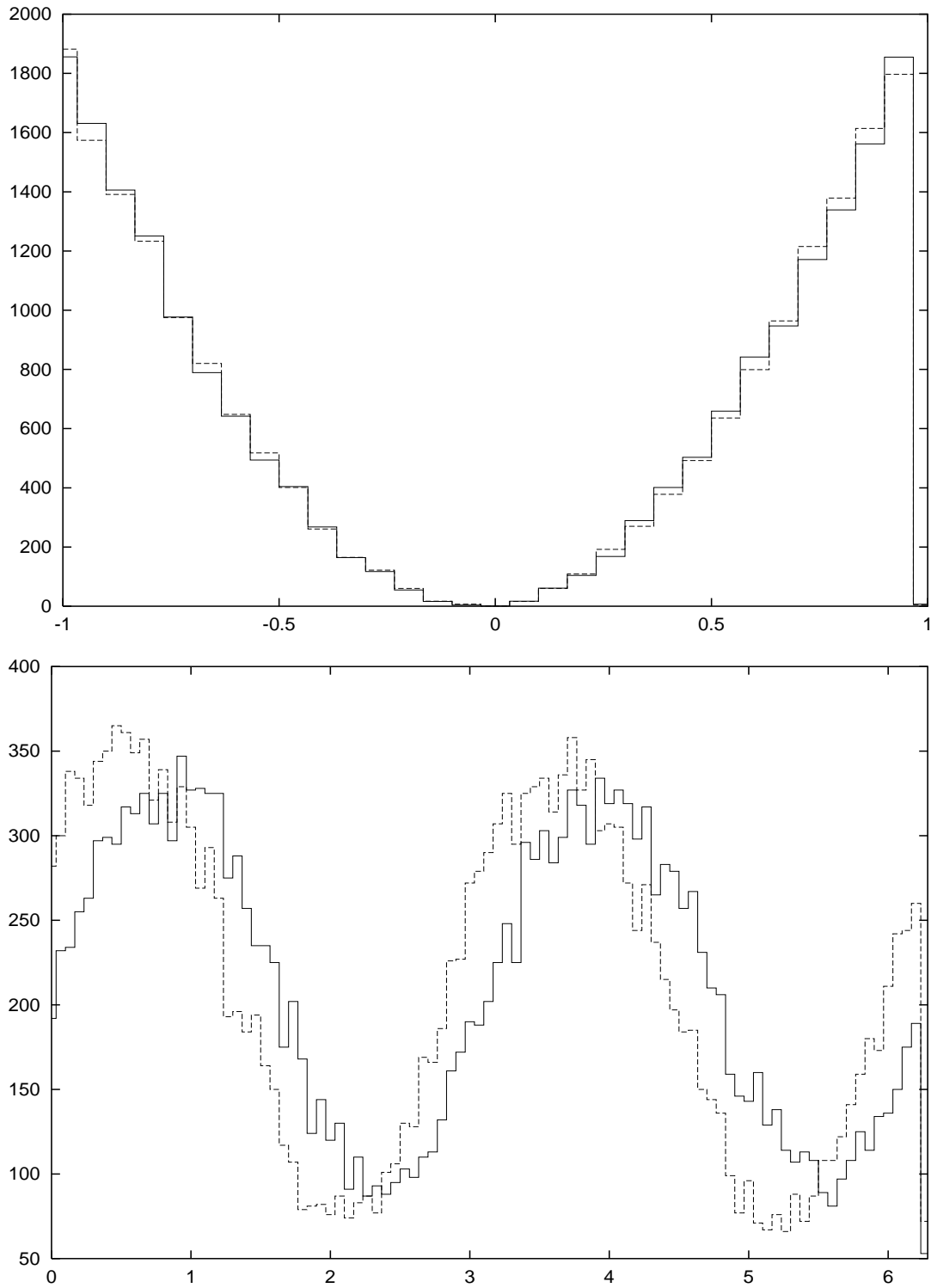


Figure 10: $\text{Cos}\theta$ distribution (upper figure) and azimuthal angle ϕ distribution (lower figure) for $\rho = 0.09, \eta = 0.323$ (full line) and $\rho = 0.254, \eta = 0.442$ (dashed line) respectively.

7 Perspectives and conclusion

- Thanks to the HQET approach and the OPE formalism which is used, we have at our disposal rigorous and *complete calculations* of the dynamics of the $B^{0\pm}$ decays into two vector mesons. This formalism is available for all charmless B decays provided the spin of the intermediate resonance(s) is less or equal 1; the only changes which must be taken into account are the V_{CKM} matrix elements, the masses and the widths of the resonances involved in each decay.

- In the case of leptonic decay of one resonance, like $J/\Psi \rightarrow e^+e^-, \mu^+\mu^-$, the angular distributions are modified because of the spin 1/2 final leptons; which require the use of other Wigner rotation matrices. Those calculations have been already done in our first paper [1].

- In the case where a $(c\bar{c})$ bound state or a charmed meson is produced like:

$$B^0 \rightarrow J/\Psi \rho^0, D^* X (X = \rho^0, \omega, K^{*0}),$$

the Wilson coefficients involved in the effective hamiltonian have to be modified, but we do not expect big change with respect to the $c_i(c'_i)$ coefficients used in the present paper.

- Other interesting consequences arise from this formalism: it can be easily extended to the numerous channels like: $B \rightarrow VP, PP$ where one or two pseudoscalar mesons ($P = 0^{-+}$) are produced directly from the B decay. Because of the simple equality $\lambda(P) = \lambda(V) = 0$, the number of helicity states is reduced from 3 to 1.

- An important point which has been mentionned in the present note is the role of the $\rho^0 - \omega$ *mixing* and its consequence for the determination of the direct CPV parameter (Section 3 and reference [7]). Tagging of B^+ and B^- is made easy thanks to the K^+ and K^- mesons coming from the cascade decays. In our opinion, we can also exploit all the angular distributions of the final particles (and their correlations) in order to detect an eventual discrepancy which can arise between the B^+ and B^- decays respectively. However, a complete study of those channels and their simulations require the knowledge of the strong phase shift δ (mentionned in Section 3) according to the $\pi\pi$ invariant mass. Work is in progress.

- Those calculations and simulations can be implemented into **SICBMC**, the Monte-Carlo generator of the LHCb experiment, in order to perform afterwards a full analysis of the simulated channels.

Acknowledgements

The authors are very grateful to Dr P.Perret, leader of the LHCb Clermont-Ferrand team, for his advices and his suggestions.

One of us (Z.J.A.) is very indebted to Professor A.W.Thomas, Director of the Special Research Centre for the Subatomic Structure of Matter, for the very exciting and illuminating discussions he got with him about the QCD penguin diagrams and their importance in the evaluation of the B^0 decay width.

This work was supported in part by the Australian Research Council and the University of Adelaide.

Appendix

A Polarizations in B_d^0 rest frame

Momentum:

$$\vec{k}_K = -\vec{k}_\rho = \vec{k} = \begin{pmatrix} k \sin \theta \cos \phi \\ k \sin \theta \sin \phi \\ k \cos \theta \end{pmatrix},$$

where θ and ϕ are respectively polar and azimuthal angles of the produced K^{*0} .

Longitudinal polarization:

$$\epsilon_K(0) = \left(\frac{|\vec{k}|}{m_K}, \frac{E_K}{m_K} \hat{k} \right), \quad \epsilon_\rho(0) = \left(\frac{|\vec{k}|}{m_\rho}, \frac{E_\rho}{m_\rho} (-\hat{k}) \right).$$

Transversal polarizations :

$$\begin{aligned} \vec{\epsilon}_K(1) &= \begin{pmatrix} \cos \theta \cos \phi \\ \cos \theta \sin \phi \\ -\sin \theta \end{pmatrix} = \vec{\epsilon}_\rho(1), \\ \vec{\epsilon}_K(2) &= \begin{pmatrix} -\sin \phi \\ \cos \phi \\ 0 \end{pmatrix} = -\vec{\epsilon}_\rho(2). \end{aligned}$$

Helicity frame :

$$\epsilon_K(+) = (\epsilon(1) + i\epsilon(2)) / \sqrt{2}, \quad \epsilon_K(-) = (\epsilon(1) - i\epsilon(2)) / \sqrt{2},$$

$$\vec{\epsilon}_K(+) = \begin{pmatrix} \cos \theta \cos \phi - i \sin \phi \\ \cos \theta \sin \phi + i \cos \phi \\ -\sin \theta \end{pmatrix} / \sqrt{2} = \vec{\epsilon}_K^*(-) = \vec{\epsilon}_\rho(-),$$

$$\vec{\epsilon}_K(-) = \begin{pmatrix} \cos \theta \cos \phi + i \sin \phi \\ \cos \theta \sin \phi - i \cos \phi \\ -\sin \theta \end{pmatrix} / \sqrt{2} = \vec{\epsilon}_K^*(+) = \vec{\epsilon}_\rho(+).$$

B Wilson's coefficients

We use, in the case of the ρ^0 production, the following linear combinations of the effective Wilson coefficients:

$$\begin{aligned} c_{t1}^\rho &= c'_1 + \frac{c'_2}{N_c}, \\ c_{p1}^\rho &= -(c'_4 + \frac{c'_3}{N_c}) + \frac{1}{2}(c'_{10} + \frac{c'_9}{N_c}), \end{aligned}$$

$$c_{p2}^\rho = \frac{3}{2} \left(c_7' + \frac{c_8'}{N_c} + c_9' + \frac{c_{10}'}{N_c} \right),$$

where c_{t1}^ρ relative to tree diagram, c_{pi}^ρ relative to penguin diagram and $0.98 < N_c < 2.01$.

When $q^2/m_b^2 = 0.3$:

$$c_1' = -0.3125, \quad c_2' = 1.1502,$$

$$c_3' = 2.443 \times 10^{-2} + 1.543 \times 10^{-3}i, \quad c_4' = -5.808 \times 10^{-2} - 4.628 \times 10^{-3}i,$$

$$c_5' = 1.733 \times 10^{-2} + 1.543 \times 10^{-3}i, \quad c_6' = -6.668 \times 10^{-2} - 4.628 \times 10^{-3}i,$$

$$c_7' = -1.435 \times 10^{-4} - 2.963 \times 10^{-5}i, \quad c_8' = 3.839 \times 10^{-4},$$

$$c_9' = -1.023 \times 10^{-2} - 2.963 \times 10^{-5}i, \quad c_{10}' = 1.959 \times 10^{-3}.$$

When $q^2/m_b^2 = 0.5$:

$$c_1' = -0.3125, \quad c_2' = 1.1502,$$

$$c_3' = 2.120 \times 10^{-2} + 2.174 \times 10^{-3}i, \quad c_4' = -4.869 \times 10^{-2} - 1.552 \times 10^{-2}i,$$

$$c_5' = 1.420 \times 10^{-2} + 5.174 \times 10^{-3}i, \quad c_6' = -5.729 \times 10^{-2} - 1.552 \times 10^{-2}i,$$

$$c_7' = -8.340 \times 10^{-5} - 9.938 \times 10^{-5}i, \quad c_8' = 3.839 \times 10^{-4},$$

$$c_9' = -1.017 \times 10^{-2} - 9.938 \times 10^{-5}i, \quad c_{10}' = 1.959 \times 10^{-3}.$$

C Form factors (BSW model)

	V	A_1	A_2
$B \rightarrow K^*$	$\frac{0.369}{1-m_\rho^2(GeV^2)/5.432(GeV^2)}$	$\frac{0.328}{1-m_\rho^2(GeV^2)/5.432(GeV^2)}$	$\frac{0.331}{1-m_\rho^2(GeV^2)/5.432(GeV^2)}$
$B \rightarrow \rho$	$\frac{0.329}{1-m_{K^*}^2(GeV^2)/5.322(GeV^2)}$	$\frac{0.283}{1-m_{K^*}^2(GeV^2)/5.322(GeV^2)}$	$\frac{0.283}{1-m_{K^*}^2(GeV^2)/5.322(GeV^2)}$

For further details, see reference [7] and literature quoted therein.

References

- [1] **Towards a unified Monte-Carlo for B meson decay simulations**
Z.J.Ajaltouni et al, LHCb 99-051, PHYSICS, December 1999.
- [2] **R.Fleischer**, private communication.
- [3] **Dynamics of the Standard Model**
Donoghue et al, Cambridge monographs on Particle Physics (1994).
- [4] **Weak Hamiltonian, CP Violation and Rare Decays**
A.J.Buras, hep-ph/9806471
("Probing the Standard Model of Particle Interactions" , F.David and R.Gupta eds, Elsevier Science).
- [5] Review of Particle Physics, **EPJC C15**, 2000.
- [6] **$\rho\omega$ mixing and direct CP violation in hadronic B decays**
S.Gardner et al, Phys.Rev.Lett. **80**, 1834 (1998) and references therein.
- [7] **Enhanced direct CP violation in $B^\pm \rightarrow \rho^0\pi^\pm$**
X.-H.Guo, O.Leitner and A.W.Thomas, Phys.Rev.D**63** (2001) 056012.
- [8] Myron Bander et al, Phs.Rev.Lett. **43** (1979) 242.
Harry Lipkin, Phy.Lett. **B 415** (1997) 186.
- [9] P.Langacker, Phys.Rev.D**20**, (1979) 2983.
- [10] **Heavy Quark Symmetry**
M.Neubert, Physics Reports **245** (1994) 259-395.
- [11] **Weak decays beyond leading logarithms**
G.Buchalla et al, Reviews of Modern Physics, Vol.68, 1125 (October 1996).
- [12] N.G.Deshpande et al, Phys.Rev.Lett. **74**, 26 (1995).
- [13] **CP Violation and the role of electroweak penguins in nonleptonic B decays**
R.Fleischer, International Journal of Modern Physics **A12**, 2459 (1997).
- [14] M.Bauer, B.Stech and M.Wirbel, Z.Phys. **C34**, 103 (1987) ;
M.Bauer et al, Z.Phys. **C29**, 637 (1985).
- [15] **Field Theory in Particle Physics**
De Wit and J.Smith, Nort-Holland (1986).
- [16] Review of Particle Physics, **EPJC C15** (2000), 110.
- [17] F.Parodi, P.Roudeau and A.Stocchi, Nuo.Cim. **A112** (1999) 833.